

# XLPE/*h*-BN Nanocomposites With Enhanced DC Insulation Properties

Shihang Wang<sup>1</sup>, Member, IEEE, Jianying Li, Senior Member, IEEE, and Shengtao Li<sup>1</sup>, Senior Member, IEEE

**Abstract**—Nanocomposites have been developed as the third-generation insulating materials. This article introduces the crosslinked polyethylene (XLPE) nanocomposite dielectric doped with a small amount of nano-hexagonal boron nitride (*h*-BN), which exhibits excellent insulation properties under high dc voltage. The test results show that XLPE/*h*-BN nanocomposites possess significant improvements in dc breakdown strength and 0.1 wt% nano *h*-BN doping can actually increase the dc breakdown strength by 39%. The space charge properties of the XLPE/*h*-BN obtained by the pulsed electro-acoustic (PEA) measurements and the direct current integrated charge [DCIC- $Q(t)$ ] measurements show that the positive homocharge injection under dc voltage is obviously suppressed, and the electrical conductivity under relatively high electric field decreases. The thermally stimulated current results show that the nano *h*-BN doping introduces only deep charge traps (above 1 eV) to the XLPE matrix. The trap energy is deeper than that of the original traps, and this is the main factor leading to the improvement of the dc insulation properties. Besides, the doping of *h*-BN does not introduce impurities or change the crystallinity of XLPE. This article presents the novel XLPE/*h*-BN nanocomposites with excellent dc insulation properties and indicates the large potential of the nano *h*-BN-doped insulation materials.

**Index Terms**—Charge injection, crosslinked polyethylene (XLPE), dc breakdown, hexagonal boron nitride (*h*-BN), nanocomposite.

## I. INTRODUCTION

NANOCOMPOSITES have excellent dielectric properties and have become the third-generation insulating materials [1]. Nano-doping can improve corona resistance and electrical tree characteristics as well as regulate dielectric properties of the polymer matrix. More importantly, the dc insulation properties can be enhanced to various degrees by inorganic nanoparticle doping, such as the suppression of the charge injection and transportation, as well as the increase of the breakdown strength. With the construction of high-voltage direct current (HVDC) transmission line in a large scale, the power industries have proposed stricter requirements on the dc insulation performance of insulating materials. Therefore,

Manuscript received May 31, 2021; accepted January 5, 2022. Date of publication January 31, 2022; date of current version March 15, 2022. This work was supported by the National Natural Science Foundation of China (NSFC) under Project 51907147 and Project U2066204. (Corresponding author: Shengtao Li.)

The authors are with the State Key Laboratory of Electrical Insulation and Power Equipment, Xi'an Jiaotong University, Xi'an, Shaanxi 710049, China (e-mail: sli@mail.xjtu.edu.cn).

Color versions of one or more figures in this article are available at <https://doi.org/10.1109/TDEI.2022.3146605>.

Digital Object Identifier 10.1109/TDEI.2022.3146605

nanocomposite dielectrics may be more suitable for dc insulation systems in the future, and nanocomposite materials with higher insulation performance need to be continuously developed. For example, crosslinked polyethylene (XLPE)-based nanocomposites are expected to be used in the new generation of HVDC cable.

XLPE nanocomposite dielectrics with inorganic oxide nanofillers, such as MgO, SiO<sub>2</sub>, Al<sub>2</sub>O<sub>3</sub>, and TiO<sub>2</sub>, have been extensively studied, for instance, the dc breakdown strength ( $E_b$ ) of XLPE can be increased by 30.0% by introduction of 2 wt% nano-SiO<sub>2</sub> [2], 29% by introduction of 3 phr nano-Al<sub>2</sub>O<sub>3</sub> [3], and 14.7% by introduction of 0.5 wt% nano-TiO<sub>2</sub> [4]. Nano-MgO is an important kind of nanofiller used to modify polyethylene, and introduction of 1 phr nano-MgO can increase the dc  $E_b$  of low-density polyethylene by 35% [5]. There are also other kinds of nanofiller applied to modulate the properties of XLPE. It has been reported that the addition of 1 wt% nano-SiC or 0.1 wt% nano-Al(OH)<sub>3</sub> can increase the dc  $E_b$  of XLPE by 27.4% and 32.2%, respectively [6]. Despite substantial amount of work has proved significant improvements in dc  $E_b$ , there are often conflicting results. For example, some articles report that the introduction of nanofillers may lead to lower dc  $E_b$  [7]. The fundamental understanding of the mechanisms involved is relatively limited.

The interphase region referring to the region between the nanofiller and the polymer matrix contains unique charge traps and limits the charge transport, and this is considered to be the main factor for regulating the dc insulation performance, for example, inhibiting the homocharge injection into the bulk from the electrodes. Several models have been proposed focusing on the trap characteristics and their influence on breakdown strength [8], [9]. Improvements of dc  $E_b$  are believed to be directly related to the deep traps enhancing the barrier height of charge injection [10], [11].

By selecting new kinds of a nanofiller, it is a way to reconstruct the charge trap distribution and shape novel and better insulation performance. Compared to other ceramic fillers, hexagonal boron nitride (*h*-BN) has high thermal conductivity, excellent high temperature resistance, sheet structure, lightweight, and moderate cost [12]. Hence micro-BN fillers have been widely used to increase the thermal conductivity of the polymer matrix [12], [13]. In this application, the BN filler content tends to be high, such as higher than 10 wt%, which may lead to the degradation of dielectric properties. The effect of low nano *h*-BN doping content on the insulation properties of XLPE has not been reported yet.

In this article, XLPE/*h*-BN nanocomposites with significantly enhanced dc insulation properties and low loading content are reported. The trap parameters, charge transport characteristics,  $E_b$  characteristics, as well as other important test results are obtained and analyzed.

## II. EXPERIMENTAL DETAILS

### A. Sample Preparation

A crosslinkable polyethylene compound (containing dicumyl peroxide crosslinking agent and antioxidant) derived from Borealis was used as the matrix. The density was  $0.92 \text{ g/m}^3$  and the melting peak temperature was  $113 \text{ }^\circ\text{C}$  measured by differential scanning calorimetry at a heating rate of  $10 \text{ }^\circ\text{C/min}$ . High pure grades of commercially nano *h*-BN filler were added by the weight ratio and its average size was 50 nm. The as-received *h*-BN was first dispersed in acetone, and an ultrasonic cell disruptor was used to make the mixed solution oscillate at a very high frequency to prevent agglomeration. In addition, a small amount of hexadecyltrimethoxysilane ( $\text{CH}_3(\text{CH}_2)_{15}\text{Si}(\text{OCH}_3)_3$ ) was added to the mixed solution to act as a dispersant. Then the processed nano *h*-BN was filtered and completely dried for later use.

A torque rheometer (HAAKE PolyLab OS) was used to disperse the nano *h*-BN filler into the crosslinkable polyethylene pellets homogeneously at a temperature of  $120 \text{ }^\circ\text{C}$ . Then film samples with different thicknesses were prepared by hot pressing under higher temperature and ensure the fully crosslinking process. Before the measurements, samples were degassed at  $70 \text{ }^\circ\text{C}$  for 24 h to exclude crosslinking by-products effectively.

Nanocomposite film samples with different nano *h*-BN content (0.1, 0.3, 0.5, 1, and 3 wt%) were prepared. For the sake of clarity, the abbreviated nomenclature will be used throughout as BN-0.1, BN-0.3, BN-0.5, BN-1, and BN-3. For accuracy of comparison, neat XLPE samples, abbreviated as XLPE, was also prepared as processed above. Nano *h*-BN dispersion in the nanocomposite sample was observed using a scanning electron microscope (SEM, Keyence VE9800). Samples with a thickness of 1 mm were broken in liquid nitrogen to obtain the cross sections. Then the cross sections were evaporated with gold before observation.

### B. FTIR and XRD Measurements

The FTIR spectra were obtained utilizing an IR Prestige-21 spectrometer with the wavenumber varying from  $3800$  to  $500 \text{ cm}^{-1}$ . The resolution was  $2 \text{ cm}^{-1}$ , and the signal was averaged with 20 scans.

The X-ray diffraction (XRD, Regaku D/MAX IIIB, Japan) was used to analyze the crystallization characteristics. The working voltage was 40 kV, and the scan ranged from  $10^\circ$  to  $30^\circ$ .

### C. DC Breakdown Measurements

A breakdown measurement setup was used to obtain dc  $E_b$  at room temperature ( $23 \pm 1 \text{ }^\circ\text{C}$ ) [6]. XLPE and nanocomposite samples were subjected to a ramp voltage with an increase

rate of  $3 \text{ kV/s}$  until breakdown phenomena happened. Sphere electrodes with a diameter of 25 mm were used, and the breakdown process was carried out in the transformer oil to prevent discharge on the sample surface. The thickness of the sample was about 0.15 mm. The data were analyzed using the Weibull distribution.

### D. Space Charge Measurements

The pulsed electro-acoustic (PEA) method was used to measure space charge distributions in XLPE and nanocomposite samples under dc voltage. The top electrode was a semiconducting electrode and the bottom electrode was aluminum. An electric pulse was applied to the sample to stimulate the space charge and to generate the acoustic signal. Silicone oil was used to act as the acoustic coupling. The space charge profiles were measured under the applied dc electric field of  $+40 \text{ kV/mm}$  at room temperature ( $23 \text{ }^\circ\text{C}$ ). The thickness of the samples was about 0.25 mm. The space charge profiles in the polarization process within 30 min were obtained. The reproducibility was confirmed by repeating the experiments for several times.

### E. Direct Current Integrated Charge Measurements

The direct current integrated charge [DCIC- $Q(t)$ ] method was used to measure the integrated current and analyze the charge transport characteristics under dc voltage [14]–[16]. The XLPE and nanocomposite films with a thickness of  $180$ – $190 \text{ }\mu\text{m}$  were chosen for the measurements. The test voltage was applying on the film sample with an electric field ranging from  $50$  to  $80 \text{ kV/mm}$ , and the charge dynamics were recorded with an interval of 2 s during the voltage application with time of 5 min by the DCIC- $Q(t)$  equipment. Typical charge injection and accumulation can be estimated based on the DCIC- $Q(t)$  results.

### F. Thermally Stimulated Current Measurements

The thermally stimulated depolarization currents (TSDCs) were measured to obtain the trap parameters and analyze their changes. A TSDC system manufactured by Novocontrol technologies GmbH & Company KG, Montabaur, Germany, was used. Samples with a thickness of about 0.28 mm were evaporated with circular gold electrodes for a good contact with the external electrodes. After that samples were poled with a  $+3\text{-kV/mm}$  dc electric field at  $70 \text{ }^\circ\text{C}$  (343 K) for 30 min in vacuum and then cooled at a rate of  $-30 \text{ }^\circ\text{C/min}$  with the poling electric field still applied. The samples were cooled to  $-150 \text{ }^\circ\text{C}$  (123 K) and shorted for 3 min. Then the currents were measured by a picoammeter (6517B, Keithley) under short circuit from  $-150 \text{ }^\circ\text{C}$  to  $130 \text{ }^\circ\text{C}$  at a rising rate of  $2 \text{ }^\circ\text{C/min}$ .

## III. RESULTS

### A. Structure Characterization

Fig. 1(a) shows the cross section of the XLPE sample, without dot-shaped impurities. Corresponding to this, it can see the dot-shaped impurities distributed on the cross section

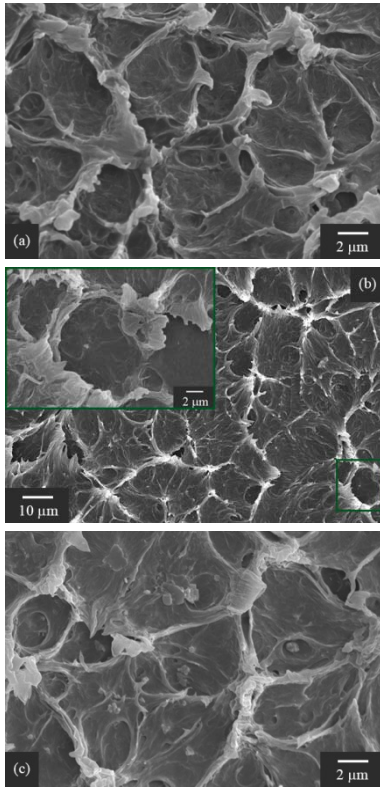


Fig. 1. SEM images of cross sections of XLPE and its nanocomposite samples. (a) XLPE, (b) BN-0.3, and (c) BN-3.

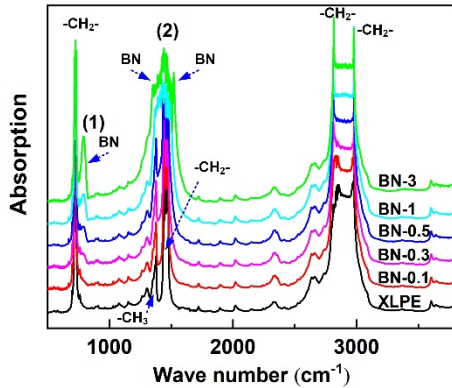


Fig. 2. Infrared spectra of XLPE and nanocomposites.

of the BN-0.3 sample [see Fig. 1(b)], representing *h*-BN particles. A larger view with a ruler of 10  $\mu\text{m}$  is placed to observe in a wider field of view. Fig. 1(c) represents the cross section of the BN-3 sample, and several agglomerates of nanofillers appear.

The infrared spectra of XLPE and XLPE/*h*-BN nanocomposite samples are shown in Fig. 2. The main differences are reflected in two regions, one is at wavenumber 790  $\text{cm}^{-1}$ , and the other is at wavenumber ranging from 1200 to 1600  $\text{cm}^{-1}$ . These changes are mainly caused by the characteristic peaks of *h*-BN and the amplitude of the infrared spectra is proportional to the nano *h*-BN content [17]. No changes of the infrared spectra are found at the other wave numbers.

Morphology of the semi-crystalline XLPE is an important factor affecting its physical properties. Fig. 3 presents the XRD curves of XLPE and XLPE/*h*-BN samples. Peak at 26.8°

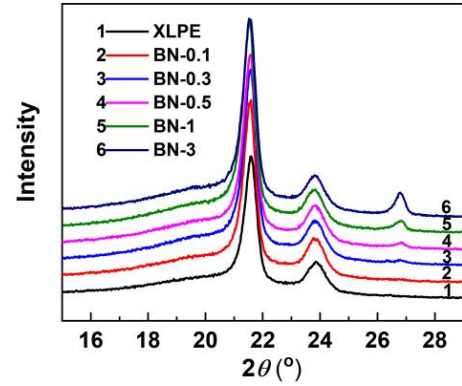


Fig. 3. XRD curves of XLPE and XLPE/*h*-BN samples.

is caused by nano *h*-BN, corresponding to the (002) crystal plane [13], [17]. It increases proportionally to the nano *h*-BN content. The principal crystalline peak of polyethylene is at 21.4°, and the secondary crystalline peak is at 23.6°, corresponded to the (110) and (220) crystal planes, respectively. It can be seen that these two peaks have no distinct differences, which indicates no distinct difference in crystallinity among these nanocomposite samples.

### B. DC Electrical Breakdown Strength

Two-parameter Weibull distribution, shown in the following equation, was used to obtain the scale parameter and the shape parameter of the dc  $E_b$ :

$$P(E_b) = 1 - \exp[-(E_b/\alpha)^\beta] \quad (1)$$

where  $P(E_b)$  is the cumulative probability,  $\alpha$  is the scale parameter, and  $\beta$  is the shape parameter of the dc breakdown field strength.

Fig. 4 shows the dc  $E_b$  Weibull distribution curve of XLPE and XLPE/*h*-BN nanocomposite samples. It presents obvious differences between samples, and the fitting has small data dispersion (95%). Fig. 5(a) gives the Weibull breakdown strength (dc  $E_b$  at  $P(E_b)$  of 63.2%) at 23 °C and it demonstrates a remarkably high  $E_b$  at the low loading contents.  $E_b$  of neat XLPE sample is 346.9 kV/mm and it increases to 481.5 kV/mm at 0.1 wt% nano *h*-BN loading. The promotion ratio reaches 39%. The dc  $E_b$  still has a 21% increase at 1 wt% nano *h*-BN loading. Even if the added content is as high as 3 wt%, the  $E_b$  of the nanocomposite is still a little bit higher than that of the neat XLPE sample. The moderate loading content of nano *h*-BN is very useful to improve the dc  $E_b$ . Fig. 5(b) shows the shape parameters of the Weibull distribution, corresponding to Fig. 4. With the increasing nano *h*-BN content, the shape parameter gradually decreases, which means the data values of dc breakdown field strength  $E_b$  are gradually scattered.

Nanocomposites containing a small amount of inorganic nanofillers have been extensively studied and proved to possess many excellent properties under dc field. The trend of dielectric strength  $E_b$  with increasing nanofiller content tends to behave in two ways. One is to rise first and then fall. The data in this article is consistent with this trend. The other is to rise first and then remains stable. This appears

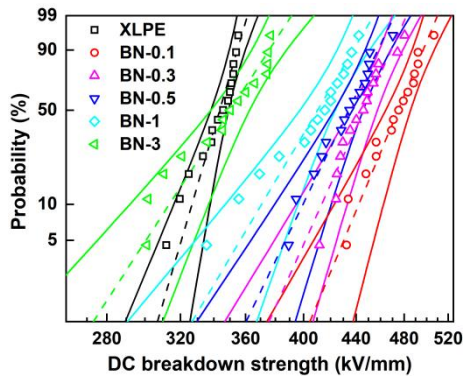


Fig. 4. Weibull distribution curve of dc breakdown strength of XLPE and nanocomposites.

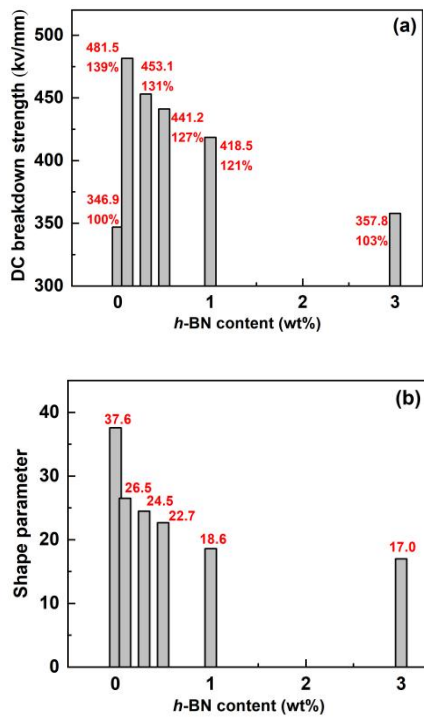


Fig. 5. DC Breakdown strength as a function of nano *h*-BN loading content. (a) Weibull breakdown strength. (b) Shape parameter.

in the results of polyethylene/MgO nanocomposites [5]. In the following research work, the authors will compare and analyze the difference between these two trends. Compared with the data mentioned in the introduction, it can be seen that a 39% increment in our work is prominent.

### C. Space Charge Properties

Under dc electric field, charge injection and space charge accumulation are important aspects to determine the dc insulation performance. Fig. 6 shows the space charge curves under +40 kV/mm within 30 min. Positive charges inject obviously in the XLPE sample from the anode as shown in Fig. 6(a). After nano *h*-BN doping, the homocharge injection is suppressed. The amount of injected charge significantly decreases in BN-0.5, BN-1, and BN-3 samples within 30 min. To be used in HVDC cable as the insulating materials, the XLPE nanocomposites should have few heterocharge caused

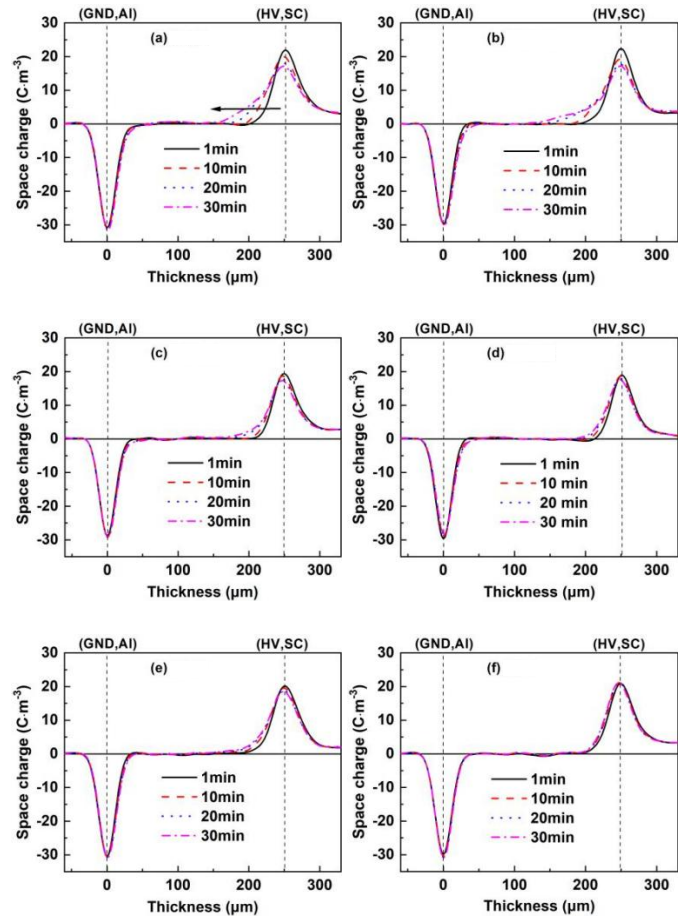


Fig. 6. Space charge curves of XLPE and nanocomposites with applied dc voltage. (a) XLPE. (b) BN-0.1. (c) BN-0.3. (d) BN-0.5. (e) BN-1. (f) BN-3.

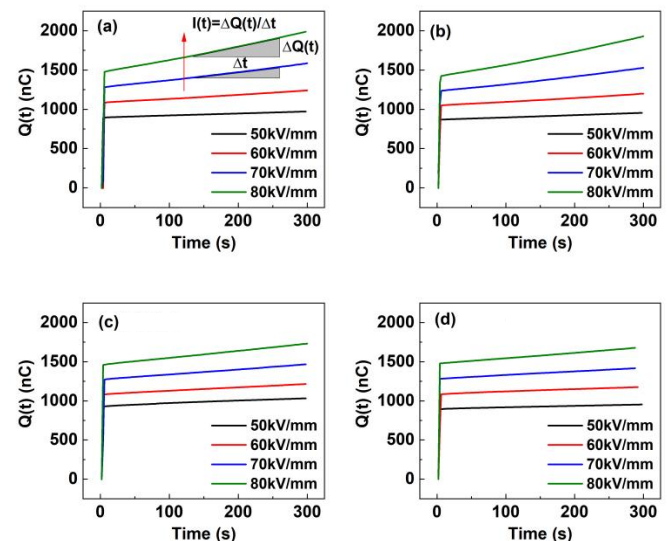


Fig. 7. DCIC- $Q(t)$  curves (the integral charge quantity) of XLPE and nanocomposites under different electric field. (a) XLPE. (b) BN-0.1. (c) BN-0.5. (d) BN-3.

by impurity ionization under dc electric field. In this article, the crosslinkable polyethylene compound pellets containing relatively low content of impurities and additives are used. So, there is few heterocharge as shown in Fig. 6.

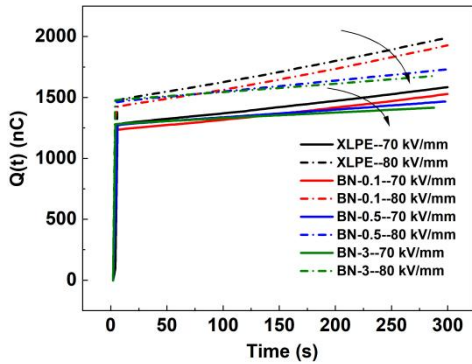


Fig. 8. Comparison of the integral charge quantity under relatively high dc electric field.

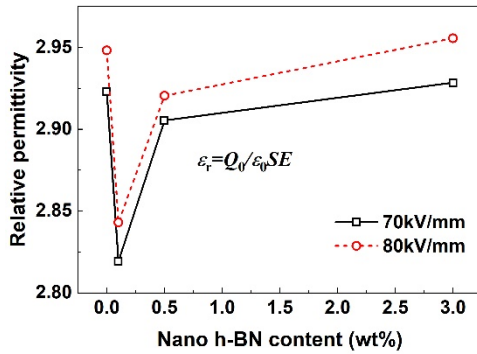


Fig. 9. Relative permittivity of XLPE and nanocomposites under high dc electric field. ( $\epsilon_r$ : dielectric constant,  $Q_0$ : initial charge,  $\epsilon_0$ : vacuum dielectric constant,  $S$ : area of the measure electrode,  $E$ : dc electric field for testing).

Fig. 7 presents the DCIC- $Q(t)$  curves that also demonstrate the effective suppression of space charge in XLPE/ $h$ -BN nanocomposite samples. It is easier to compare the changing trends when the curves of the samples are drawn together, as shown in Fig. 8. The charge injection and charge migration in XLPE has been significantly suppressed by the nano  $h$ -BN. The black arrows in Fig. 8 indicate that as the doping content of nano  $h$ -BN increases, the amount of  $Q(t)$  decreases.

The electrical conduction currents  $I(t)$  can be calculated by differentiating  $Q(t)$  as shown in Fig. 7(a). In Fig. 8, it can be seen that  $I(t)$  also significantly reduces with increasing nano  $h$ -BN content as the black arrows show. In addition, the initial  $Q(t)$  value after the instantaneous polarization is completed ( $Q_0$ ) of BN-0.1 sample is relatively lower at 70 and 80 kV/mm. It is believed that this phenomenon is caused by the lower relative permittivity ( $\epsilon_r$ ) of the BN-0.1 sample comparing to the other samples. According to the relation between  $Q_0$  and  $\epsilon_r$ ,  $\epsilon_r$  of XLPE and XLPE/ $h$ -BN samples were obtained, as shown in Fig. 9.

#### D. Trap Characteristics

Fig. 10 shows the TSDC curves of the XLPE and XLPE/ $h$ -BN nanocomposite samples. As widely accepted, the polyethylene displays three current peaks in the TSDC curve. In Fig. 10, the  $\gamma$  peak is relatively not obvious and appears below  $-100$  °C. The  $\beta$  peak shows at  $-43$  °C and is not distinctly influenced by the nano  $h$ -BN doping. What changes

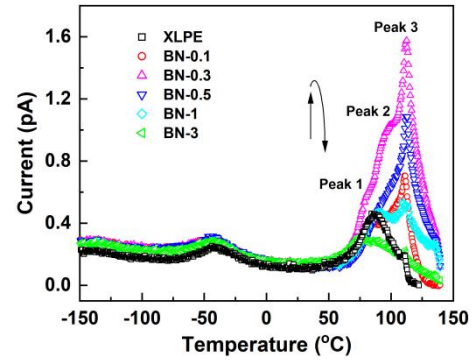


Fig. 10. Thermally stimulated depolarizing current curves of XLPE and XLPE/ $h$ -BN nanocomposite samples.

TABLE I  
TRAP LEVEL ENERGY OF XLPE AND XLPE  
NANOCOMPOSITE SAMPLES

Samples	Peak1		Peak 2		Peak 3	
	$T_p/K$	$E_T/eV$	$T_p/K$	$E_T/eV$	$T_p/K$	$E_T/eV$
XLPE	362	0.93	/	/	/	/
BN-0.1	356	1.10	373	1.70	385	3.1
BN-0.3	356	1.20	372	1.70	386	3.1
BN-0.5	357	1.30	372	1.60	386	3.1
BN-1	355	1.05	376	1.75	389	2.9

significantly is the  $\alpha$  peak at about 110 °C. The  $\alpha$  peak splits into three peaks: peak 1, peak 2, and peak 3. Peak 2 is obscured by the other two stronger peaks and is not obvious except in the BN-0.3 sample. The three peak values increase first and then decrease with the increasing loading content. The highest current value appears in BN-0.3. The energy levels of the charge traps can be obtained by fitting experimental results of TSDC curves using the following equation [18]:

$$I(T) = B \exp \left[ -\frac{E_T}{k_B T} - \frac{1}{\beta \tau_0} \int_{T_0}^T \exp \left( -\frac{E_T}{k_B T'} \right) dT' \right] \quad (2)$$

where  $I(T)$  is the TSDC current in pA.  $B$  is a constant.  $E_T$  is the activation energy of the relaxation process in eV, which is regarded as the trap level energy.  $\beta$  is the heating rate in  $K \cdot s^{-1}$ .  $\tau_0$  is the relaxation time constant in s.  $k_B$  is Boltzmann's constant.  $T$  is the temperature in K.

The calculated trap levels are shown in Table I. Since the amplitudes of the three peaks of BN-3 are difficult to estimate, the calculation results of its trap level energy may be inaccurate and are not listed here. It can be concluded that deep traps are mainly introduced into XLPE/ $h$ -BN nanocomposites.

Since the integrated area of the current peak is related to the trap density, it can be considered that the charge trap density first increases and then decreases with the increase of nano  $h$ -BN doping content.

#### IV. DISCUSSION

$h$ -BN is widely used in polymer composites and mainly to improve the thermal conductivity. In this case, a large amount of micrometer-sized boron nitride is often used [19]. Besides,  $h$ -BN is a good insulating dielectric with a wide bandgap energy (ranging from 5 to 6 eV [20], [21]) and a high dc

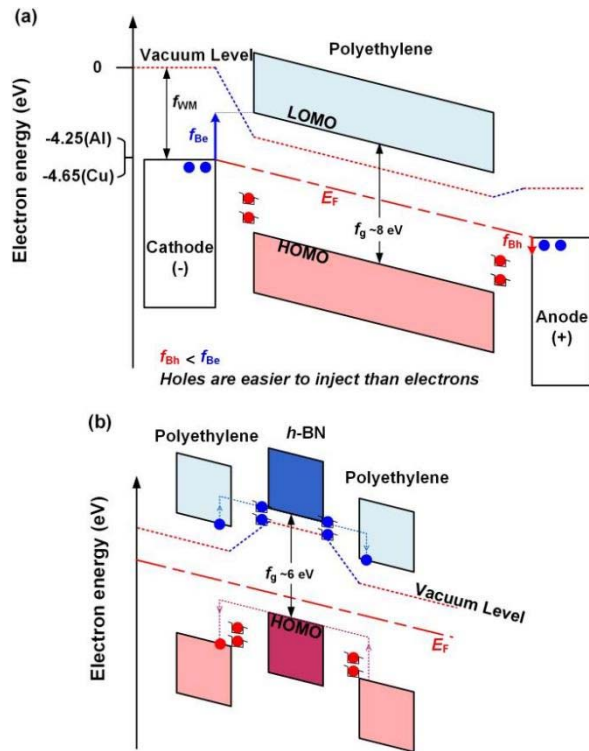


Fig. 11. Diagram of the energy level and charge exchange in the XLPE/*h*-BN samples. (a) At the electrode/sample interface. (b) In the bulk.

$E_b$  ( $E_{b//c} = \sim 12$  MV/cm,  $E_{b\perp c} = \sim 3$  MV/cm [22]). In this article, nano-scale *h*-BN is used as a filler to regulate the dc insulation performance of XLPE. Polyethylene has a wide bandgap of  $\sim 8$  eV, and its calculated Fermi energy level is about  $-2.85$  or  $-3.16$  eV [23], which is higher than that of the electrodes (Al  $-4.25$  or Cu  $-4.65$  eV). Thus, the charge exchange occurs at the electrode/sample interface to form an electric double layer. As shown in Fig. 11(a), this makes the injection barrier of holes lower, and holes are easier to inject from the anode. Hole injection at the anode is more readily facilitated than electron injection at the cathode in polyethylene and this is consistent with the PEA results, as shown in Fig. 6. The Fermi energy level of the *h*-BN surface layer is about  $-4.6$  eV [21]. The Fermi energy level balance of the interface between the polyethylene and *h*-BN also makes the charge exchange and forms an electric double layer, that is, the surface layer of *h*-BN negatively charged, and the polyethylene layer forms the positively charged local state, as shown in Fig. 11(b). In this way, *h*-BN forms hole traps and traps the injected holes that migrate under the dc electric field and hence the hole mobility is reduced significantly. The hole traps are also the important reason for the inhibition of the homocharge injection. Besides, *h*-BN forms energy barriers which will also hinder the migration of electrons.

For the ion carrier conduction in the matrix, it will also be blocked by the nano *h*-BN when the ion carriers move along the intermolecular region. In addition, *h*-BN has a typical sheet structure and will likely be oriented along with the extension of the sheet samples in the hot-pressing process. Then the blocking effect for ion carriers may be stronger. On the other

hand, the larger specific surface area of the nanofiller enhances the restriction on the movement of the molecular chain, which is proved by the decreased relative permittivity as shown in Fig. 9. From this perspective, the restriction of molecular chain movement also limits the transport of ion carriers.

Under the dc electric field, the inhibited charge injection, the suppressed charge transport, and the decreased relative permittivity are all the causes of the improved dc  $E_b$  [24], [25]. High dc  $E_b$  at a low doping content is the most important feature of the XLPE/*h*-BN nanocomposites. The addition of nano *h*-BN only significantly introduced very deep traps for XLPE, which is also a distinctive feature. Although the prominent deep trap characteristics can give the improvement of dc insulation performance, there are still other factors influencing the test results.

The first is that the trap characteristics and the charge transport characteristics show a more complicated relationship. The trap density varies obviously in samples, increasing first and then decreasing, and the maximum value appears in the BN-0.3 sample. The charge injection or conduction results do not present the similar maximum phenomenon; instead, it shows a monotonic relationship with the increasing nanofiller content. The second is that, generally speaking, the homocharge injection is suppressed, which tends to increase the dc  $E_b$ . But  $E_b$  shows a maximum value in the BN-0.1 sample. This is inconsistent with the monotonous change of the charge injection behavior. The third is that some experimental results indicate that the density of deep traps tend to have a positive correlation with the dc  $E_b$ , but the maximum values are at 0.3 and 0.1 wt% content, respectively. This is mainly related to the dispersion of nanoparticles and caused by the influence of the nanoparticle agglomeration.

It should be noted that, as the nano *h*-BN content increase, to avoid the agglomeration of nanofillers in the melt blending process is more difficult. As shown in Fig. 1, the agglomerated size of the nanofiller increases significantly when the nano *h*-BN content reaches 3 wt%, reaching a maximum size close to  $\sim 1$   $\mu\text{m}$ . The nanofiller agglomeration means more physical defects, which will degrade the dielectric strength to a certain extent and cause the increased dispersion of the dc  $E_b$ , leading to the decrease in the shape parameter as shown in Fig. 5(b). It needs to explore better surface functionalization treatment methods to improve the dispersion of nano *h*-BN in the polyethylene matrix later.

## V. CONCLUSION

The XLPE/*h*-BN nanocomposite with high dc breakdown strength and suppressed charge injection features were introduced in this study. It is useful to reach the conclusions as follows.

1) XLPE/*h*-BN nanocomposite samples with loading content ranging from 0.1 to 3 wt% were prepared successfully. The dc  $E_b$  of the nanocomposite sample shows at most a 39% increase under 0.1 wt% loading.

2) The effect of *h*-BN doping on the charge trap characteristics of XLPE is a significant increase in the density of deep traps, and this is the main cause for the improvement of dc insulation properties.

3) The positive homocharge injection and transport shows dominating position in the neat XLPE sample and this effect was obviously suppressed by the nano *h*-BN doping.

## REFERENCES

- [1] S. Li, S. Yu, and Y. Feng, "Progress in and prospects for electrical insulating materials," *High Voltage*, vol. 1, no. 3, pp. 122–129, Oct. 2016.
- [2] L. Zhang *et al.*, "Effect of nanoparticle surface modification on breakdown and space charge behavior of XLPE/SiO<sub>2</sub> nanocomposites," *IEEE Trans. Dielectr. Electr. Insul.*, vol. 21, no. 4, pp. 1554–1564, Aug. 2014.
- [3] Y. Park *et al.*, "DC conduction and breakdown characteristics of Al<sub>2</sub>O<sub>3</sub>/cross-linked polyethylene nanocomposites for high voltage direct current transmission cable insulation," *Jpn. J. Appl. Phys.*, vol. 53, no. 8S3, pp. 08NL05-1–08NL05-6, 2014.
- [4] S. Wang, P. Chen, S. Yu, P. Zhang, J. Li, and S. Li, "Nanoparticle dispersion and distribution in XLPE and the related DC insulation performance," *IEEE Trans. Dielectr. Electr. Insul.*, vol. 25, no. 6, pp. 2349–2357, Dec. 2018.
- [5] Y. Murakami *et al.*, "DC conduction and electrical breakdown of MgO/LDPE nanocomposite," *IEEE Trans. Dielectr. Electr. Insul.*, vol. 15, no. 1, pp. 33–39, Feb. 2008.
- [6] S. Wang, P. Chen, J. Xiang, and J. Li, "Study on DC breakdown strength and morphology in XLPE/Al(OH)<sub>3</sub> nanocomposites," in *Proc. Int. Symp. Electr. Insulating Mater. (ISEIM)*, Sep. 2017, pp. 355–358.
- [7] K. Y. Lau, A. S. Vaughan, G. Chen, I. L. Hosier, A. F. Holt, and K. Y. Ching, "On the space charge and DC breakdown behavior of polyethylene/silica nanocomposites," *IEEE Trans. Dielectr. Electr. Insul.*, vol. 21, no. 1, pp. 340–351, Feb. 2014.
- [8] S. Li, G. Yin, S. Bai, and J. Li, "A new potential barrier model in epoxy resin nanodielectrics," *IEEE Trans. Dielectr. Electr. Insul.*, vol. 18, no. 5, pp. 1535–1543, Oct. 2011.
- [9] T. Tanaka, M. Kozako, N. Fuse, and Y. Ohki, "Proposal of a multi-core model for polymer nanocomposite dielectrics," *IEEE Trans. Dielectr. Electr. Insul.*, vol. 12, no. 4, pp. 669–681, Aug. 2005.
- [10] S. Li, "Charge dynamics: Linking traps to insulation failure," in *Proc. IEEE 11th Int. Conf. Properties Appl. Dielectr. Mater. (ICPADM)*, Jul. 2015, pp. 1–14.
- [11] S. Wang, P. Chen, H. Li, J. Li, and Z. Chen, "Improved DC performance of crosslinked polyethylene insulation depending on a higher purity," *IEEE Trans. Dielectr. Electr. Insul.*, vol. 24, no. 3, pp. 1809–1817, Jun. 2017.
- [12] W. Zhou, S. Qi, Q. An, H. Zhao, and N. Liu, "Thermal conductivity of boron nitride reinforced polyethylene composites," *Mater. Res. Bull.*, vol. 42, no. 10, pp. 1863–1873, Oct. 2007.
- [13] T. Zhao and X. Zhang, "Enhanced thermal conductivity of PE/BN composites through controlling crystallization behavior of PE matrix," *Polym. Compos.*, vol. 38, no. 12, pp. 2806–2813, Dec. 2017.
- [14] S. Yu *et al.*, "Surface trap effects on flashover voltages of epoxy/Al<sub>2</sub>O<sub>3</sub> nanocomposites for high voltage insulation," *J. Mater. Sci., Mater. Electron.*, vol. 30, no. 19, pp. 18135–18143, Oct. 2019.
- [15] Y. Sekiguchi *et al.*, "A study on electric charge behaviors in polymeric materials using 'direct current Integrated charge method'," in *Proc. Int. Symp. Elect. Insul. Mater. (ISEIM)*, 2017, pp. 691–694.
- [16] W. Wang, K. Sonoda, S. Yoshida, T. Takada, Y. Tanaka, and T. Kurihara, "Current integrated technique for insulation diagnosis of water-tree degraded cable," *IEEE Trans. Dielectr. Electr. Insul.*, vol. 25, no. 1, pp. 94–101, Feb. 2018.
- [17] H. Harrison *et al.*, "Quantification of hexagonal boron nitride impurities in boron nitride nanotubes via FTIR spectroscopy," *Nanosci. Adv.*, vol. 1, no. 5, pp. 1693–1701, 2019.
- [18] J. Turnhout, *Thermally Stimulated Discharge of Electrets*. Berlin, Germany: Springer, 1980, pp. 173–191.
- [19] J. Chen, X. Huang, B. Sun, and P. Jiang, "Highly thermally conductive yet electrically insulating polymer/boron nitride nanosheets nanocomposite films for improved thermal management capability," *ACS Nano*, vol. 13, no. 1, pp. 337–345, Jan. 2019.
- [20] K. Watanabe, T. Taniguchi, and H. Kanda, "Direct-bandgap properties and evidence for ultraviolet lasing of hexagonal boron nitride single crystal," *Nature Mater.*, vol. 3, no. 6, pp. 404–409, Jun. 2004.
- [21] S. Ogawa, T. Yamada, R. Kadowaki, T. Taniguchi, T. Abukawa, and Y. Takakuwa, "Band alignment determination of bulk *h*-BN and graphene/*h*-BN laminates using photoelectron emission microscopy," *J. Appl. Phys.*, vol. 125, no. 14, Apr. 2019, Art. no. 144303.
- [22] K. Nagashio *et al.*, "Electrical integrity and anisotropy in dielectric breakdown of layered *h*-BN insulator," *ECS Trans.*, vol. 79, no. 1, pp. 91–97, May 2017.
- [23] W. Wang, T. Takada, Y. Tanaka, and S. Li, "Trap-controlled charge decay and quantum chemical analysis of charge transfer and trapping in XLPE," *IEEE Trans. Dielectr. Electr. Insul.*, vol. 24, no. 5, pp. 3144–3153, Oct. 2017.
- [24] W. Wang, D. Min, and S. Li, "Understanding the conduction and breakdown properties of polyethylene nanodielectrics: Effect of deep traps," *IEEE Trans. Dielectr. Electr. Insul.*, vol. 23, no. 1, pp. 564–572, Feb. 2016.
- [25] S. Wang, S. Yu, J. Xiang, J. Li, and S. Li, "DC breakdown strength of crosslinked polyethylene based nanocomposites at different temperatures," *IEEE Trans. Dielectr. Electr. Insul.*, vol. 27, no. 2, pp. 482–488, Apr. 2020.



**Shihang Wang** (Member, IEEE) was born in Shaanxi, China, in 1990. He received the B.S. and Ph.D. degrees in electrical engineering from Xi'an Jiaotong University, Xi'an, China, in 2012 and 2018, respectively.

He is currently an Assistant Professor with the State Key Laboratory of Electrical Insulation and Power Equipment, Xi'an Jiaotong University. His research interests include insulation materials especially the cable insulating materials and nanocomposites.



**Jianying Li** (Senior Member, IEEE) was born in Shaanxi, China, in 1972. He received the B.S., M.S., and Ph.D. degrees in electrical engineering from Xi'an Jiaotong University, Xi'an, China, in 1993, 1996, and 1999, respectively.

He is currently a Professor with Xi'an Jiaotong University. His research interests include high-voltage insulation and dielectrics.



**Shengtao Li** (Senior Member, IEEE) received the Ph.D. degree in electrical engineering from Xi'an Jiaotong University (XJTU), Xi'an, China, in 1990.

He was a Lecturer, an Associate Professor, and a Professor with XJTU, in 1990, 1993, and 1998, respectively. From 1993 to 2003, he was also the Deputy Director of the State Key Laboratory of Electrical Insulating and Power Equipment (SKLEIPE), XJTU. He was also a Research Fellow with Waseda University, Tokyo, Japan, in 1996. He was also a Senior Visiting Scholar with the University of Southampton, Southampton, U.K., in 2001. Since 2003, he has been an Executive Deputy Director of SKLEIPE. His research interests include dielectrics and their application, insulating materials, and electrical insulation.

Dr. Li was awarded a Distinguished Young Scholar of China by the National Science Foundation in 2006. He gave Liu Ziyu Memorial Lecture on the 11th International Conference on the Properties and Applications of Dielectric Materials (ICPADM) in 2015. He was the Chair of the 6th International Conference on Conditional Monitoring and Diagnosis (CMD) in 2016; the 1st International Conference on Electrical Materials and Power Equipment (ICEMPE) in 2017, the 2nd ICEMPE in 2019, and the 3rd ICEMPE in 2021; the 12th International Conference of Properties and Applications of Dielectric Materials (ICPADM) in 2018; and the 22th International Symposium on High Voltage Engineering (ISH) in 2021.